CrystEngComm

Accepted Manuscript

ROYAL SOCIETY OF CHEMISTRY

www.rsc.org/crystengcomm

One-pot, template-free syntheses of spherical ZnS nanocrystals using a new S^{2-} source and their photocatalytic study

Manjodh Kaur, Nipun Kumar Gupta and C. M. Nagaraja*

Department of Chemistry, Indian Institute of Technology Ropar, Rupnagar 140001, Punjab, India. **Email:** cmnraja@iitrpr.ac.in, Tel:+91-1881242229

Abstract

A facile, one-pot synthesis of template-free ZnS microspheres composed of nanocrystals (NCs) have been successfully synthesized by solvothermal method using 4,4'-dibenzyldisulfide (DBDS = $(C_7H_7)_2S_2$)) as a new temperature controlled in situ source of S^{2-} ions without (**S1-S3**) and with the use of capping agent (**S4**). The powder X-ray diffraction measurements of all the four (**S1**-**S4**) samples revealed the cubic or zinc blende (ZB) structure of the ZnS microspheres. FESEM analyses showed almost spherical morphology of the ZnS microspheres which are composed of smaller NCs. TEM analyses of the samples **S3** and **S4** confirmed the ZnS microspheres with assembled NCs. Optical measurements of the samples (**S1-S4**) showed blue-shift in the UV-vis absorption maxima compared to that of bulk ZnS due to quantum confinement effect. Photoluminescence measurements show intense blue emission of the samples. Photocatalytic investigation of the uncapped (**S3**) and mercaptoethanol (MCE)-capped (**S4**) ZnS microspheres for degradation of methylorange (MO) revealed higher photocatalytic activity of **S3** over **S4** under UV light irradiation. The lower catalytic activity of **S4** has been attributed due to the presence of MCE capping agents which acts as a barrier for the interaction of MO molecules with the ZnS NCs. The proposed mechanism for the formation of ZnS microspheres and their photocatalytic activity has also been presented.

1. Introduction

Semiconductor nanocrystals (NCs) continue to attract immense attention due to their unique optical, electrical and catalytic properties.[1] Among the various semiconductor nanomaterials, ZnS with its large direct band gap of 3.66 eV at 27°C is one of the important II-VI group semiconductor with potential applications in optoelectronic and luminescent devices.[2] ZnS exists in two different polymorphic structures namely cubic zinc-blende (ZB) structure and the hexagonal wurtzite (WZ) structure.[3] Between these, the most stable form in the bulk is the cubic or ZB structure which transforms into a thermodynamically meta stable state called the hexagonal WZ structure at temperature of 1020°C. Previously reported studies have shown that the properties of nanomaterials depend on their crystallite's size, shape and structure.[4] Therefore, synthesis of semiconductor NCs with deterministic control over the size, shape and phase is crucial for realizing their multifunctional nanodevice applications.[5] In this context, extensive efforts have been reported on controlled synthesis of ZnS nanostructures with various morphologies such as, spheres, rods, flowers, sheets, etc.[6, 7] The formation of these nanostructures has been mostly driven by self-assembly processes and assisted by template molecules/capping agents. On the other hand, the organic capping ligand-free NCs offer several advantages over capped-NCs.[8] However, it is quite challenging to develop ligand-free routes for synthesis of semiconductor NCs with controlled size and shape.[9]

Several organosulfur compounds such as, thiourea, thioacetamide, L-cysteine, etc have been utilized as in situ source of S^{2-} ions for the synthesis of phase pure ZnS nanostructures.[7] However, the literature survey on ZnS nanostructures synthesized from various organosulfur sources revealed that it is quite difficult to obtain NCs with ultrasmall (~ 2 nm) size without the use of template/capping ligand (Table 1). It has been suggested that for synthesizing nanomaterials with controlled size, it is necessary to separate the nucleation stage from the growth step.[10] In this context, we thought that use of organosulfur compounds with temperature controlled release of S^{2-} ions would be beneficial for controlling the growth of NCs. Our previous attempts in these lines on utilizing temperature controlled sulfur source resulted semiconductor NCs with ultrasmall (2-5 nm) size without the use of template/capping ligand. In continuation of our efforts, we investigated for the first time the utility of DBDS (dibenzyl disulphide = $(C_7H_7)_2S_2$) with temperature controlled release of S^{2-} ions for the synthesis of phase pure ZnS nanostructures. In support of this, we have been able synthesize ZnS NCs with smaller (3-6 nm) crystallite's size highlighting the merits of DBDS as sulfur source. Herein, we report the synthesis, characterization and photocatalytic activity

of phase pure cubic ZnS NCs of 3-6 nm size using DBDS as a new in situ source of S^{2-} ions without the use of template/capping agent (**S1-S3**). Further, to study the effect of capping agents[8] on the crystallite size, shape and the photocatalytic activity of ZnS NCs, we have also synthesized mercaptoethanol (MCE) capped cubic ZnS NCs (**S4**). Optical measurements of the samples (**S1-S4**) showed blue-shift in the UV-vis absorption maxima compared with that of bulk ZnS due to quantum confinement effect. Photocatalytic investigation of both uncapped (**S3**) and MCE-capped (**S4**) ZnS microspheres for degradation of MO under UV light irradiation revealed higher photocatalytic activity of **S3** over **S4**. The relatively lower photocatalytic activity of **S4** has been attributed due to the effect of MCE capping agents which acts as a barrier for the interaction of MO molecules with the ZnS NCs. The unique features of the synthetic procedure followed here are a facile, template-free, one-pot route for synthesis of phase pure ZnS NCs with high yield and almost uniform morphology.

2. Experimental

All the starting materials were commercially available and used as received without further purification. $Zn(NO_3)_2.6H_2O$ and 4,4'-dibenzyl disulphide (DBDS) were purchased from Sigma–Aldrich Chemical Co. Methyl orange (MO) was purchased from Alfa Aesar.

2.1 Synthesis of ZnS microspheres

The ZnS microspheres (**S1-S4**) were synthesized by solvothermal route as follows. To a 6 mL DMF solution of $Zn(NO_3)_2.6H_2O$ (0.029 g, 0.1 mmol), 3 ml ethanolic solution of DBDS (0.024 g, 0.1 mmol) was added. The mixture with a solvent ratio 2:1 was stirred for 15 minutes and then transferred into a stainless steel teflon lined autoclave and heated at 180°C for 6.5 hrs. After being cooled to room temperature naturally a white precipitate was collected by centrifugation and thoroughly washed with methanol then the products were dried under vacuum (yield of **S1**:80%). Samples, **S2** and **S3** were prepared by following the procedure similar to **S1**, except that the reaction temperature was maintained at 200°C (yield of **S2**:72%) and 220°C (yield of **S3**:70%) respectively. The MCE-capped ZnS sample (**S4**) was prepared by using the procedure similar that of **S3** except that, the synthesis was carried out in the presence of 5 equivalents (1 mmol, 35μL) of MCE capping agent (yield of **S4**:75%)

2.2 Characterization

Powder X-ray diffraction (XRD) patterns of the as-prepared samples were recorded on a PANalytical's X'PERT PRO diffractometer. Field-emission scanning electron microscopy (FESEM) images were recorded on a Carl zeiss ultra 55 FE SEM. Transmission electron microscopy (TEM), high-resolution TEM (HRTEM) and selected area electron diffraction (SAED) measurements were recorded on JEOL JEM-2100F Field Emission TEM. UV–vis

spectra were recorded on a Perkin Elmer Model Lambda 900 spectrophotometer. Fourier-transform infrared (FT-IR) measurements were recorded on Bruker TENSOR-27 spectrometer. Photoluminescence measurements were recorded at room temperature on a Perkin Elmer LS55 fluorescence spectrophotometer.

2.3 Photocatalytic investigation

Photocatalytic activity of the as-prepared samples of ZnS microspheres for the photocatalytic degradation of an aqueous solution of MO was carried out as follows. As-prepared sample of ZnS microspheres (**S3/S4**) (40 mg) was suspended in a solution of MO (5.0×10^{-5} M) in 50 mL of H_2O in a quartz tube at ambient temperature. A 400 W high pressure mercury lamp was used as the UV-vis light source. The lamp was equipped with double walled quartz jacket for constant water circulation and as a water filter to remove the heating effects. The distance between the UV light source and the quartz reaction tube was maintained at 13 cm. Before irradiation, the mixture was stirred well in the dark for 30 minutes to establish an adsorption–desorption equilibrium between the ZnS NCs and MO then the photocatalytic reaction was initiated. The reaction was started after the intensity of the mercury lamp became stable. At regular time intervals, aliquots of the sample were withdrawn and the catalyst was separated through centrifugation and analyzed for MO dye concentration. The percentage degradation of MO dye was determined using the following relation.

$$\% \text{ Degradation} = (C_i - C_f)/ C_i$$

where, C_i and C_f are the initial and final concentrations of MO, respectively

3 Results and Discussions

3.1 Synthesis and Characterization

As mentioned before, the ZnS NCs (**S1-S4**) were synthesized by solvothermal route using DBDS as an *in situ* sulfur source. For the sake of comparison, we have tabulated some of the literature reports of ZnS nanostructures synthesized using various organosulfur sources (Table 1).[11] It is evident from the Table 1 that hardly there have been any reports of synthesis of ZnS NCs with smaller crystallite's size (2-5 nm) in the absence of a template/capping ligand. On the contrary, our synthesis route resulted ZnS NCs with ultrasmall (~ 2nm) size even in the absence of any stabilizing ligand. Further, the synthesis can be carried out in air to obtain phase pure ZnS NCs with high yield and almost uniform morphology.

Powder XRD pattern of the as-prepared samples of ZnS microspheres (**S1**-**S4**) are shown in Fig.1(a). The diffraction peaks were observed at $2\theta = 29.07°$, 48.31° and 56.77° which can be assigned due to (111), (220) and (311) planes of cubic or ZB structure of ZnS (JCPDS

reference card no. 5-556). The broadness of the diffraction peaks suggest the finite size of these crystallites. The absence of any additional diffraction peaks corresponding to either $Zn(NO_3)_2$ or any other impurities indicate high purity of the sample. The mean crystallite's size (D) of the NCs calculated using the Scherer equation, $D = 0.94\lambda/B\cos\theta$ (where, D = crystallite size, λ = wavelength of X-ray (1.540598 Å), B = value of full width at half maxima (FWHM) and θ is the Bragg's angle) are 2.34, 5.92, 6.66 and 3.66 nm for the samples **S1**, **S2**, **S3** and **S4**, respectively. The composition of the samples (**S1**-**S4**) was determined by energy dispersive X-ray spectroscopy (EDX). As shown in the Fig. 1b only peaks due to Zn^{2+} and S^{2-} were observed for the uncapped sample **S3**. Whereas the MCE-capped sample, **S4** shows additional peaks originating from oxygen and carbon atoms of MCE capping agent. The quantitative analysis confirmed the atom ratio of Zn^{2+}/S^{2-} to be 1:1. Furthermore, FT-IR spectra of the uncapped sample **S3** shows only the stretching bands due to the solvent molecules and in case of sample **S4**, additional stretching bands at 2879, 2809, 1104, 1038 and 695 cm^{-1} corresponding to C-H, S-H, C-O, C-C and C-S stretching frequencies were observed due to MCE-capping agent, (Figs. S1 and S2, ESI). Thus, the above mentioned analyses clearly support the formation of uncapped (**S1-S3**) and MCE-capped (**S4**) ZnS microspheres with phase pure cubic ZB structure.

The morphology of the as-prepared samples, **S1**-**S4** was examined by FESEM and TEM analyses. As shown in Fig. 2 FESEM images of all the samples show the presence of almost uniform solid spheres with diameters in the range of 0.35 to 1.2 μm. The broad size distribution of ZnS microspheres particularly in case of samples **S1**-**S3** can be attributed to self-agglomeration of NCs due to the absence of capping agent. Moreover, the magnified FESEM images of individual ZnS microspheres of the samples **S1**-**S4** unveiled the presence of assembled smaller NCs (Fig. 3). Furthermore the precise value of the crystallite's size was determined by TEM analyses. Fig.4a shows the low-magnification bright-field TEM image of a single uncapped ZnS microsphere, **S3** whose size is about 400 nm. The TEM image of a selected region on the surface of the sphere shows the presence of ZnS NCs whose crystallite size lie in the range of 6-10 nm (inset of Fig. 4a) which is in near agreement with the crystallite's size value calculated from XRD (ca. 6.66 nm). The diffraction planes obtained from the SAED pattern match well with the XRD patterns (Fig. 4b). HRTEM image shows structurally uniform lattice fringes of ZnS NCs suggesting crystalline nature of the sample and the calculated fringe spacing of 0.31 nm corresponds to the (111) lattice plane of cubic ZnS (Fig. 4c). Fig. 5a shows low-magnification bright-field TEM image of a single MCE-capped ZnS microspheres, **S4** with a size distribution of about 360 nm. The TEM image of a

selected region on the surface of the sphere shows the presence of ZnS NCs whose crystallite's size lie in the range of 4-8 nm (inset of Fig.5a), which is in line with the value of crystallite size calculated from XRD (ca. 3.66 nm). The diffraction planes obtained from the SAED pattern match with the XRD patterns (Fig.5b). HRTEM image shows structurally uniform lattice fringes of ZnS NCs, suggesting crystalline nature of the material and the calculated fringe spacing of 0.31 nm corresponds to the (111) lattice plane of the cubic structure of ZnS (inset (c) of Fig. 5). Therefore, the above mentioned data strongly supports the formation of ZnS NCs.

3.2 Formation of ZnS microspheres

The formation of ZnS microspheres can be explained as shown in Scheme 1. In situ generation of S^{2-} ions by the C–S and S-S bond cleavage of DBDS linker at temperatures of 180-220 ^{o}C followed by reaction with Zn^{2+} ion to form ZnS NCs. Then self-aggregation of these NCs results in the formation of ZnS microspheres as depicted in Scheme 1. Here, DBDS molecule acts as a clean source of S^{2-} ions which are released in a controlled fashion by in situ cleavage of C–S and S-S bonds. Therefore the formation of ZnS microspheres **S1**-**S4** is driven by self-aggregation of individual ZnS NCs due to surface energy minimization as shown in Scheme 1.

3.3 Optical properties

The room temperature UV-vis absorption spectra of ZnS microspheres **S1**–**S4** dispersed in methanol is shown in Fig. 6. The spectra show sharp band edge absorptions in the UV region with absorption maxima at 240, 275, 280 and 255 nm for **S1**, **S2**, **S3** and **S4**, respectively. The blue shift in the absorption edge of the NCs in comparison with that of bulk ZnS (334 nm) can be attributed due to quantum confinement effect.[12] Similar observation of blue-shift in the absorption edge for ZnS microspheres has been reported[13] suggesting that the UV-vis absorption mainly depends on the size of primary particles and the hierarchical ZnS microspheres exhibit the activity of their nanoscale building blocks. The values of direct band gap energy (E_g) of ZnS NCs was estimated from a plot of $(\alpha h\nu)^2$ vs photon energy ($h\nu$) following the Tauc relationship,[14] $\alpha h\nu = A(h\nu - E_g)^n$ where, $h\nu$ = photon energy, A = constant, α = absorption coefficient, $\alpha = 4\Pi k/\lambda$; k is the absorption index, λ is the wavelength and n depends on the type of transition, n=1/2 for the allowed direct band gap.[15] The direct band gap values estimated by extrapolating the absorption edge by a linear fitting method were 5.00, 4.25, 4.61 and 4.92 eV for sample **S1, S2, S3** and **S4**, respectively (Fig S2).

3.4 Photoluminescence studies

Photoluminescence spectra of as-synthesized ZnS samples (**S1-S4**) dispersed in methanol were recorded at room temperature. As shown in the Fig. 7 intense blue emission with maxima cantered around 450 nm along with two shoulder peaks located around 385 and 466 nm were observed with the excitation wavelength of 240, 275, 280 and 255 nm for **S1**, **S2**, **S3** and **S4** respectively. Similar observation of multiple emission bands from ZnS samples has been reported earlier.[6a] In our studies, the dominant blue emission observed around 450 nm can be assigned due to the recombination of free charge carriers at the surface defect sites of the ZnS. Furthermore, the weak shoulder peaks located around 385 nm and 466 nm can be attributed due to sulphur and zinc vacancies, respectively. Similarly, Hu and co-workers have reported ZnS nanobelts that show fluorescence emission band at 401 nm along with shoulder peak at 470 nm when excited with 250 nm.[16] Kar and Chaudhuri have reported the synthesis of wurtzite ZnS nanostructures that exhibit an intense blue emission consisting of two bands at 394 and 456 nm when excited again at 250 nm wavelength.[17] Moreover, it has also been reported that ZnS microspheres that display strong blue emission band around 415 nm with weak shoulder peak appearing at 466 nm wavelength.[18]

3.5 Photocatalytic activity of ZnS NCs

The degradation of toxic and non-biodegradable organic dyes using nanomaterials has attracted significant current interest for the removal of environmental pollutants from waste water.[19] In this regard, photocatalytic activity of uncapped (**S3**) and MCE-capped (**S4**) ZnS NCs was investigated for degradation of MO in aqueous solution under UV light irradiation. MO dye was chosen for the study since it is one of the major organic pollutants from textile and dyeing industries.[20] Furthermore, it is a carcinogenic and resistant to direct degradation by sunlight or ultraviolet light. However, it can be photoreduced to harmless organic compounds using photocatalysts. The degradation can be easily monitored with decrease in the intensity of the characteristic absorption band at 463 nm. To rule out the possibility of decolouration by UV light, blank experiments were carried out in the absence of the catalyst which showed negligible degradation of MO suggesting the necessity of catalyst for the degradation process. Figs. 8a and b show the changes in the optical absorption spectra of MO at different time intervals under UV light irradiation catalyzed by ZnS NCs. As it can be seen, with increase in irradiation time the concentration of MO decreases and at the end of 120 min the % degradation of MO was found to be 80.0% and 71.0% catalyzed by un-capped (**S3**) and MCE-capped (**S4**) ZnS NCs, respectively indicating higher photocatalytic performance of **S3** over **S4** (Fig. 8c). The relatively lower photocatalytic activity of **S4** can be attributed due to the effect of MCE capping agents which acts as a barrier for the interaction of MO molecules

with the ZnS NCs. Furthermore, the kinetics of photocatalytic degradation of MO using ZnS NCs can be best explained using pseudo first order reaction, $\ln(C_o/C_t) = K_{app}t$ where, C_o is the concentration of dye after keeping in darkness after 30 min and C_t is the concentration of dye at given time interval t. The plot of $\ln(C_o/C_t)$ vs t is shown in Fig. 8d. The estimated value of rate constant for the photocatalytic reaction catalyzed by uncapped (**S3**) and MCE-capped (**S4**) ZnS samples are 1.278 x 10^{-2} and 1.033 x 10^{-2} min^{-1} respectively supporting higher catalytic activity of **S3** over **S4**. Similar observation of higher catalytic activity of uncapped NCs over organic ligand-capped semiconductor NCs for the photocatalytic degradation of MO has been observed before.[9] The catalytic activity of ZnS NCs observed here is comparable or higher than some of the reported examples of ZnS nanostructures utilized for photocatalytic degradation of MO (Table. 2)[21] Moreover, the catalytic rate is also comparable to the best known ultraviolet light photocatalyst, ZnO whose rate constant for catalytic degradation of MO is reported to be 1.7 x 10^{-2} m^{-1}.[22]

In order to determine the stability and recyclability of the catalysts, the ZnS samples (**S3** and **S4**) were isolated after the catalytic cycle by centrifuging the dispersed solution and washing several times with methanol. The powder XRD spectra of the recycled samples match very well with those of original samples confirming the photostability and recyclability of both uncapped (**S3**) and MCE-capped (**S4**) ZnS samples (Fig. S7)

3.6 Proposed mechanism for the degradation of MO

The general mechanism of photocatalysis involves absorption of photons by semiconducting material (here ZnS) leading to photoexcitation of electrons from the valence band (VB) to the conduction band (CB) to generate electron–hole (e_{CB}^-/h_{VB}^+) pair (eqn (1)).[23]

$$ZnS + h\nu \longrightarrow (e_{CB}^-)_{ZnS} + (h_{VB}^+)_{ZnS} \qquad (1)$$

Then the photogenerated electron–hole pair migrates to the surface of the catalyst (ZnS) and reacts with the adsorbed dye molecules on the surface (eqn (2)–(5)). Followed by transfer of the photogenerated electrons to the dye molecules which is crucial for increasing the activity of a photocatalyst by inhibiting electron–hole recombination

$$O_2 + ZnS\,(e_{CB}^-) \longrightarrow O_2^{\bullet -} \quad (2)$$

$$O_2 + 2(e_{CB}^-)_{ZnS} + 2H^+ \longrightarrow H_2O_2 \quad (3)$$

$$(e_{CB}^-)_{ZnS} + O_2^{\bullet -} + 2H^+ \longrightarrow HO^\bullet + HO^- \quad (4)$$

$$H_2O + (h_{VB}^+)_{ZnS} \longrightarrow HO^\bullet + H^+ \quad (5)$$

The reactive species ($O_2^{\bullet -}$, $^\bullet OH$) produced as shown in the eqns (2)–(5) can react with MO to form the degradation products through several possible pathways as has been proposed before eqn (6) (see Scheme S1, ESI).[24]

$$MO + (O_2^{\bullet -}, HO^\bullet)/H_2O_2 \longrightarrow \text{degradation product} \quad (6)$$

The observed difference in the photocatalytic activity of uncapped (**S3**) and MCE-capped (**S4**) ZnS NCs can be explained as follows. The ZnS NCs in both **S3** and **S4** are quite active and can produce the electron–hole pairs under UV light irradiation but their contact with air is obstructed by the presence of MCE-capping agents in case of **S4**. The MCE capping agents act as physical barrier for MO molecules from easy access to catalytically active ZnS NCs in case of **S4**. Whereas, in the case of **S3** the MO molecules can easily access to the surface of ZnS NCs and can interact with the charge carriers (electrons and holes) which is a crucial step in the degradation process. This phenomena clearly supports the relatively higher rate of photocatalytic degradation of MO with uncapped ZnS NCs, **S3** (1.278×10^{-2}) as compared to that of MCE-capped ZnS NCs, **S4** (1.033×10^{-2}).

Furthermore, it is noteworthy that the absorption edge of MO shows blue shift to shorter wavelength as shown in Fig.8. This phenomenon suggests that during the course of photocatalysis the MO molecules were oxidized and converted into molecules with lower degree of Π-Π conjugation. The absorption maxima (λ_{max}) of these molecules produced during the degradation of MO is shorter than that of original MO molecules. Further oxidation leads to opening of aromatic rings and consequently to degradation of MO to CO_2 and H_2O (Scheme S1, ESI†).

Conclusions

In summary, a facile, one pot, template-free route for synthesis of uncapped (**S1-S3**) and MCE-capped (**S4)** ZnS microspheres composed of NCs (3-6 nm) has been developed. For the

first time, dibenzyl disulphide (DBDS) has been utilized as a temperature controlled in situ source of S^{2-} ions for the formation of ZnS NCs. A possible mechanism for the formation of ZnS microspheres has also been proposed. Photocatalytic investigation of both uncapped (**S3**) and MCE-capped (**S4**) ZnS microspheres revealed very good photocatalytic activity for the degradation of MO under UV light irradiation. The photocatalytic activity of uncapped ZnS NCs (**S3**) is higher compared to that of MCE-capped ZnS microspheres (**S4**). The lower photocatalytic performance of **S4** has been attributed to the presence of MCE capping agents which acts as a barrier for the interaction of dye molecules with ZnS NCs. Thus the effect of capping agent on the photocatalytic activity of ZnS NCs has been demonstrated. These results demonstrate the significance of developing capping ligand-free NCs for catalytic applications.

ACKNOWLEDGMENT

CMN gratefully acknowledges the financial support from the Department of Science and Technology (DST) and the Council of Scientific & Industrial Research (CSIR), Government of India. The authors thank the director IIT Ropar for the encouragement.

References

1. (a) A. P. Alivisatos, *Science*., 1996, **271**, 933; (b) X. Chen, A. C. S. Samia, Y. Lou and C. Burda, *J. Am. Chem. Soc.*, 2005, **127**, 4372; (c) M. A. El-Sayed, *Acc. Chem. Res.*, 2004, **37**, 326; (d) R. Jose, N. U. Zhanpeisov, H. Fukumura, Y. Baba and M. Ishikawa, *J. Am. Chem. Soc.*, 2005, **128**, 629; (e) R. Jose, Z. Zhelev, R. Bakalova, Y. Baba and M. Ishikawa, *Appl. Phys. Lett.*, 2006, **89**, 013115; (f) K. P. Kadlag, M. J. Rao and A. Nag, *J. Phys. Chem. Lett*, 2013, **4**, 1676; (g) P. V. Kamat, *Acc. Chem. Res.*, 2012, **45**, 1906; (h) C. B. Murray, D. J. Norris and M. G. Bawendi, *J. Am. Chem. Soc.*, 1993, **115**, 8706; (i) A. Nag and D. D. Sarma, *J. Phys. Chem. C*, 2007, **111**, 13641; (j) A. Puzder, A. Williamson, F. Gygi and G. Galli, *Phys. Rev. Lett.*, 2004, **92**, 217401; (k) S. Sapra, S. Mayilo, T. A. Klar, A. L. Rogach and J. Feldmann, *Adv. Mater.*, 2007, **19**, 569.
2. (a) Y. C. Cao and J. Wang, *J. Am. Chem. Soc.*, 2004, **126**, 14336; (b) X. Fang, T. Zhai, U. K. Gautam, L. Li, L. Wu, Y. Bando and D. Golberg., *Prog. Mater Sci.*, 2011, **56**, 175; (c) F. -J. Fan, L. Wu and S.-H. Yu, *Energ. Environ. Sci.*, 2014, **7**, 190; (d) C. A. Feigl, A. S. Barnard and S. P. Russo, *CrystEngComm.*, 2012, **14**, 7749; (e) A. K.

Kole, C. S. Tiwary and P. Kumbhakar, *J. Mater. Chem. C.*, 2014, **2**, 4338; (f) X. Wang, J. Shi, Z. Feng, M. Li and C. Li, *Phys. Chem. Chem. Phys.*, 2011, **13**, 4715; (g) T. Zhai, L. Li, Y. Ma, M. Liao, X. Wang, X. Fang, J. Yao, Y. Bando and D. Golberg, *Chem. Soc. Rev.*, 2011, **40**, 2986.

3. (a) S. Acharya, N. Maheshwari, L. Tatikondewar, A. Kshirsagar and S. Kulkarni, *Cryst. Growth. Des.*, 2013, **13**, 1369; (b) S. Biswas and S. Kar, *Nanotechnology.*, 2008, **19**, 045710; (c) N. S. Karan, S. Sarkar, D. Sarma, P. Kundu, N. Ravishankar and N. Pradhan, *J. Am. Chem. Soc.*, 2011, **133**, 1666; (d) Z. Wang, L. L. Daemen, Y. Zhao, C. S. Zha, R. T. Downs, X. Wang, Z. L. Wang and R. J. Hemley, *Nat Mater.*, 2005, **4**, 922.
4. (a) L. Manna, D. J. Milliron, A. Meisel, E. C. Scher and A. P. Alivisatos, *Nat Mater.*, 2003, **2**, 382; (b) L. Manna, E. C. Scher and A. P. Alivisatos, *J. Am. Chem. Soc.*, 2000, **122**, 12700; (c) Z. A. Peng and X. Peng, *J. Am. Chem. Soc.*, 2001, **123**, 183; (d) G. Schmid, *Chem. Rev.*, 1992, **92**, 1709; (e) D. V. Talapin, A. L. Rogach, A. Kornowski, M. Haase and H. Weller, *Nano Lett.*, 2001, **1**, 207; (f) C. B. Murray, D. J. Norris and M. G. Bawendi, *J. Am. Chem. Soc.*, 1993, **115**, 8706.
5. (a) P. Brown and P. V. Kamat, *J. Am. Chem. Soc.*, 2008, **130**, 8890; (b) M. Bruchez, M. Moronne, P. Gin, S. Weiss and A. P. Alivisatos, *Science.*, 1998, **281**, 2013; (c) X. Gao, Y. Cui, R. M. Levenson, L. W. Chung and S. Nie, *Nat. Biotechnol.*, 2004, **22**, 969; (d) V. Wood, J. E. Halpert, M. J. Panzer, M. G. Bawendi and V. Bulovic, *Nano Lett.*, 2009, **9**, 2367.
6. (a) S. Li, Z. Wu, W. Li, Y. Liu, R. Zhuo, D. Yan, W. Jun and P. Yan, *CrystEngComm.*, 2013, **15**, 1571; (b) S. K. Panda and S. Chaudhuri, *J. Colloid Interface Sci.*, 2007, **313**, 338; (c) N. Shanmugam, S. Cholan, N. Kannadasan, K. Sathishkumar and G. Viruthagiri, *Solid State Sci.*, 2014, **28**, 55.
7. (a) F. Davar, M. Mohammadikish, M. R. Loghman-Estarki and Z. Hamidi, *CrystEngComm.*, 2012, **14**, 7338; (b) H. Tong, Y.-J. Zhu, L.-X. Yang, L. Li, L. Zhang, J. Chang, L.-Q. An and S.-W. Wang, *J. Phys. Chem. C.*, 2007, **111**, 3893; (c) Y. Zhao, Y. Zhang, H. Zhu, G. C. Hadjipanayis and J. Q. Xiao, *J. Am. Chem. Soc.*, 2004, **126**, 6874.
8. N. Zhiqiang and L. Yadong, *Chem. Mater.*, 2014, **26**, 72.
9. (a) M. Kaur and C. M. Nagaraja, *RSC Adv.*, 2014, **4**, 18257; (b) C. M. Nagaraja and M. Kaur, *Mater. Lett.*, 2013, **111**, 230.

10. (a) R. Viswanatha and D. D. Sarma, in Nanomaterials Chemistry, Wiley-VCH Verlag GmbH & Co. KGaA, 2007, DOI: 10.1002/9783527611362.ch4, pp. 139; (b) D. Pan, Q. Wang and L. An, *J. Mater. Chem.*, 2009, **19**, 1063.
11. (a) Luo, Duan, M. Ye, Zhang and Li,*J. Phys. Chem. C.*, 2008, **112**, 2349; (b) S. K. Panda and S. Chaudhuri, *J. Colloid. Inter. Sci.*, 2007, **313**, 338; (c) X. Wang, F. Wan, K. Han, C. Chai and K. Jiang, *Mater. Charact.*, 2008, **59**, 1765; (d) S. Emin, D. Lisjak, M. Pitcher and M. Valant, *Micropor. Mesopor. Mater.*, 2013, **165**, 185; (e) Q. Wang, Z. Xu, H. Yin and Q. Nie, *Mater. Chem. Phys.*, 2005, **90**, 73; (f) Q. Zhao, Y. Xie, Z. Zhang and X. Bai, *Cryst. Growth Des.*, 2006, **7**, 153; (g) X. Wu, K. Li and H. Wang, *J. Alloys. Compd.*, 2009, **487**, 537; (h) A. Sobhani, M. Salavati-Niasari and M. Sobhani*, Mater. Sci. Semicond. Process.,* 2013, **16**, 410; (i) K. V. Anand, M. K. Chinnu, R. M. Kumar, R. Mohan and R. Jayavel, *J. Alloys Compd*., 2010, **496**, 665; (j)M. Jayalakshmi and M. M. Rao, *J. Power Sources*., 2006, **157**, 624.
12. H. Weller, *Angew. Chem. Int. Ed.*, 1993, **32**, 41.
13. N. A. Dhas, A. Zaban and A. Gedanken, *Chem. Mater.*, 1999, **11**, 806.
14. (a) S. Baskoutas, A. F. Terzis and W. Schommers, *J. Comput. Theor. Nanosci.*, 2006, **3**, 269; (b) N. Bouropoulos, I. Tsiaoussis, P. Poulopoulos, P. Roditis and S. Baskoutas, *Mater. Lett.*, 2008, **62**, 3533; (c) Fang, U. K. Gautam, Y. Bando, B. Dierre, T. Sekiguchi and D. Golberg, *J. Phys. Chem. C.*, 2008, **112**, 4735.
15. (a) S. Kar and S. Chaudhuri, *J. Phys. Chem. B.*, 2005, **109**, 3298; (b) N. Serpone, D. Lawless and R. Khairutdinov, *J. Phys. Chem.*, 1995, **99**, 16646; (c) Q. Xiong, G. Chen, J. D. Acord, X. Liu, J. J. Zengel, H. R. Gutierrez, J. M. Redwing, L. C. Lew Yan Voon, B. Lassen and P. C. Eklund, *Nano Lett.*, 2004, **4**, 1663.
16. P. Hu , Y. Liu , L. Fu , L. Cao , and D. Zhu *J. Phys. Chem. B.*, 2004, **108**, 936.
17. S. Kar and S. Chaudhuri,*J. Phys. Chem. B.,* 2005, **109**, 3298.
18. Q. Wu, H. Cao, S. Zhang, X. Zhang, and D. Rabinovich, *Inorg Chem.*, 2006, **45**, 7316.
19. (a) S. Kundu, *Colloid Surface A.*, 2014, **446**, 199; (b) S. Kundu, M. D. Mukadam, S. M. Yusuf and M. Jayachandran, *CrystEngComm.*, 2013, **15**, 482; (c) S. Kundu, S. Panigrahi, A. Pal, S. K. Ghosh, S. Nath, S. Praharaj, S. Basu and T. Pal, *Dyes. Pigments.*, 2006, **69**, 177.
20. (a) S.K. Kansal , M. Singh , D. Sud,*J. Hazard. Mater*., 2007,**141**, 581; (b) A. Kar, Y. R. Smith and V. Subramanian, *Environ. Sci.Technol*., 2009, **43**, 3260.

21. (a) Y. Lixiong, W. Dan, H. Jianfeng, C. Liyun, O. Haibo, W. Jianpeng and Y. Xiang, *Ceram. Int.*, 2015, **41**, 3288; (b) Z. Liu, D. Zhang, H. Yang and R. He, *Mater. Sci. Semicond. Process.,* 2013, **16**, 1779; (c) S. Joicy, R. Saravanan, D. Prabhu, N. Ponpandian and P. Thangadurai, *RSC Adv.*, 2014, **4**, 44592; (d)F. Chen, Y. Cao and D. Jia, *Chem.Engg. J.*, 2013, **234**, 223.

22. (a) H. Zhang and Y. Zhu, *J. Phys. Chem. C.*, 2010, **114**, 5822; (b)Luo, Duan, M. Ye, Zhang and Li, *J. Phys. Chem. C.*, 2008, **112**, 2349; (c) Q. Wu, H. Cao, S. Zhang, X. Zhang and D. Rabinovich, *Inorg. Chem.*, 2006, **45**, 7316; (d) Y. F. Zhu, D. H. Fan and W. Z. Shen, *Langmuir.*, 2008, **24**, 11131; (e) E.-K. Maged, E.-S. Hany, J. *Photochem. Photobiol. A: Chem.*, 2009, **205,** 151; (f)X. Li, C. Hu, H. Liu, J. Xu, B. Wan, X. Wang, *Physica E.*, 2011, **43,** 1071.

23. (a) P. Raja, A. Bozzi, H. Mansilla, and J. Kiwi,*J. Photochem. Photobiol. A.*, 2005, **169**, 271; (b) M. Stylidi, D. I. Kondarides and X. E. Verykios, *Appl. Catal. B.*, 2004, **47**, 189; (c)A. H. Boonstra and C. A. H. A. Mutsaers, *J. Phys. Chem.*, 1975, **79**, 1940;(d) I. K. Konstantinou and T. A. Albanis, *Appl. Catal. B: Environ.*, 2004, **49**, 1; (e) D. Xiang, Y. Zhu, C. Cai, Z. He, Z. Liu, D. Yin, J. Luo, *Physica E.*, 2011,**44**, 733; (f)A. C. Herath, R. M. G. Rajapakse, A. Wicramasinghe and V. Karunaratne., *Environ. Sci. & Tech.*, 2008, **43**, 176;(g) R. Vinu and G. Madras, Environ. Sci. Technol., 2009, **43**, 473.

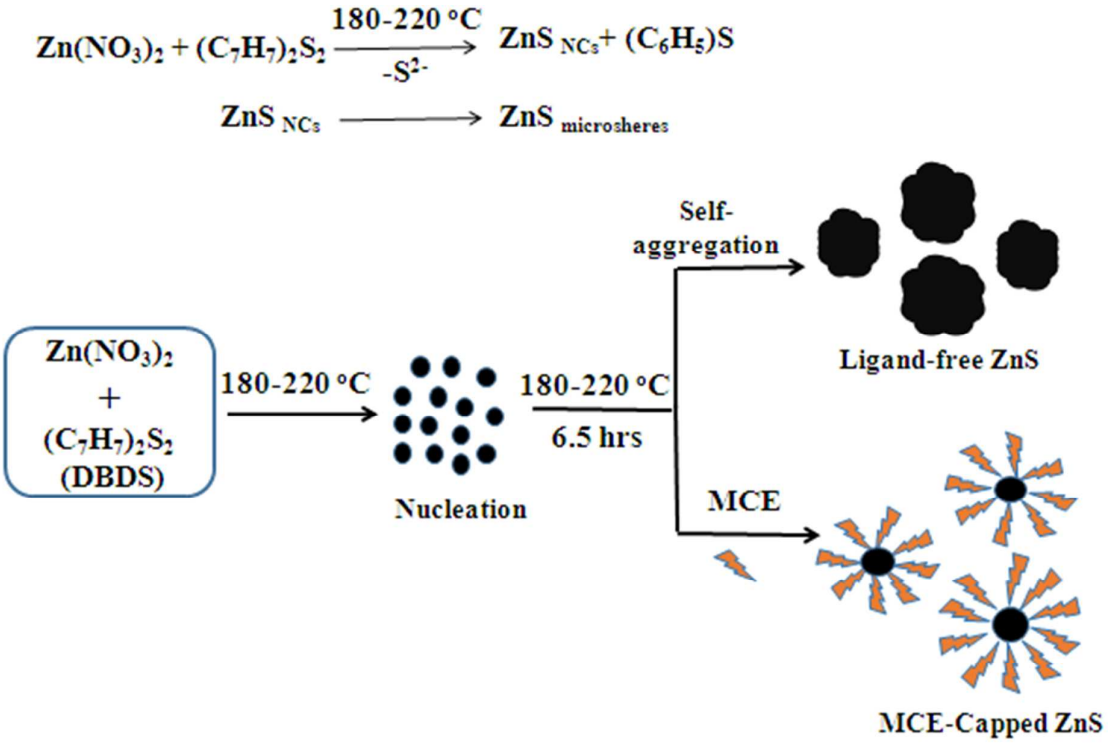

Scheme1. The proposed mechanism for the formation of ZnS microspheres

Table 1. Comparison chart for synthesis of ZnS NCs using various organosulphur sources

S. No.	Metal precursor	Sulphur source	Capping agent/ Template	Temperature (^oC)	Crystallite size (nm)	Reference
1	$Zn(acac)_2$	Thioacetamide	Thioglycolic acid	110-180	10-27	7(a)
2	$Zn(NO_3)_2.6H_2O$	Thioacetamide	Polyethylene glycol	200	20	11(a)
3	$Zn(NO_3)_2.6H_2O$	Thioacetamide	Sodium EDTA	130-230	20-25	11(b)
4	$Zn(SO_4)_3$	Thiourea	PVP	150	12.3	11(c)
5	$Zn(CH_3COO)_2.2H_2O$	Thiourea	Ethylenediamine	180	12-20	11(d)
6	$ZnCl_2$	Thiourea	Ethylenediamine	180	40	11(e)
7	$Zn(CH_3COO)_2.2H_2O$	Thiourea	Thioglycolic acid	180	20	11(f)
8	$Zn(CH_3COO)_2.2H_2O$	L-Cysteine	Granular Gelatin	100	10-40	11(g)
9	$[Zn(TSC)_2]\ Cl_2$	Thiosemicarbazide	Oleylamine	150	11	11(h)
10	$Zn(CH_3COO)_2.2H_2O$	Thiosemicarbazide	Hexamethylenetetraamine (HMTA)	180	2-3	11(i)
11	$Zn(NO_3)_2.6H_2O$	Thiourea	No capping agent /template	170	9.3-12.7	11(j)
12	$Zn(NO_3)_2.6H_2O$	Dibenzyl disulphide (DBDS)	No capping agent/ template	180-220	2.3-6.6	This work

Table 2. Comparison of rate constant (*k*) values for catalytic degradation of MO by ZnS NCs.

S. No.	Catalyst	Sulphur source	Temperature of syntheses (^oC)	Conc. of dye solution	Catalyst loading	Rate constant (*K*) value	Reference
1	Ligand free ZnS NCs	Thioacetamide	170	10 mgL^{-1}	1.0 gL^{-1}	4.98 x 10^{-2} m^{-1}	21(a)
2	Ligand free ZnS NCs	Thiourea	170	10 mgL^{-1}	1.0 gL^{-1}	3.90 x 10^{-2} m^{-1}	21(a)
3	Ligand free ZnS NCs	Commercially bought ZnS	Microwave synthesis	20 mgL^{-1}	0.05 gL^{-1}	7.55 x 10^{-3} m^{-1}	21(b)
4	Thiogylcollic acid-capped ZnSnanorods	Thioacetamide	100	10 mgL^{-1}	0.2 gL-1	1.17x 10^{-2} m^{-1}	21(c)
5	Ligand free ZnS NCs	Dibenzyl disulphide (DBDS)	220	16 mgL^{-1}	0.8 gL^{-1}	1.03 x 10^{-2} m^{-1}	This work
6	MCE-capped ZnS NCs	DBDS	220	16 mgL^{-1}	0.8 gL^{-1}	1.27 x 10^{-2} m^{-1}	This work

Figures with captions

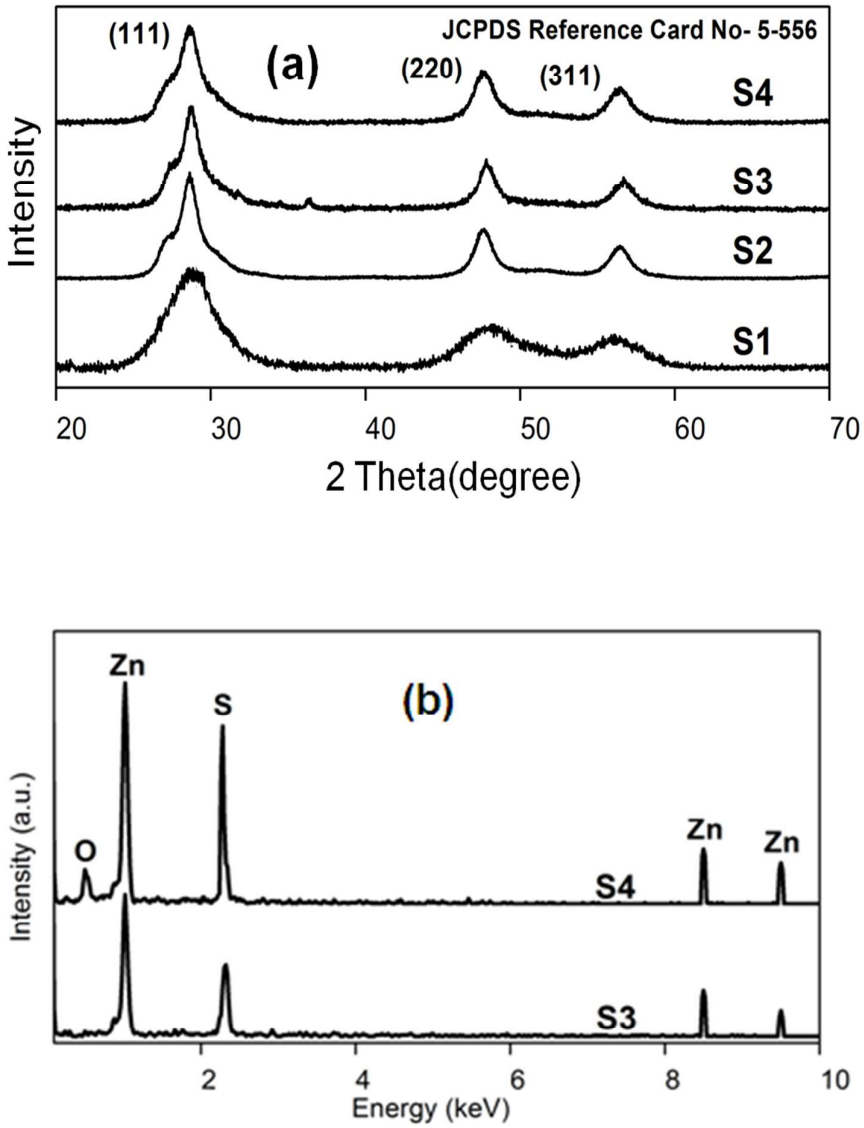

Fig. 1 (a) XRD patterns of the as-prepared ZnS microspheres at temperatures of 180° (**S1)** 200° (**S2**), 220°C (uncapped, **S3)** and 220°C (MCE-capped, **S4**). (b) EDS spectra of the as-prepared sample of uncapped (**S3)** and MCE-capped (**S4)** ZnS microspheres.

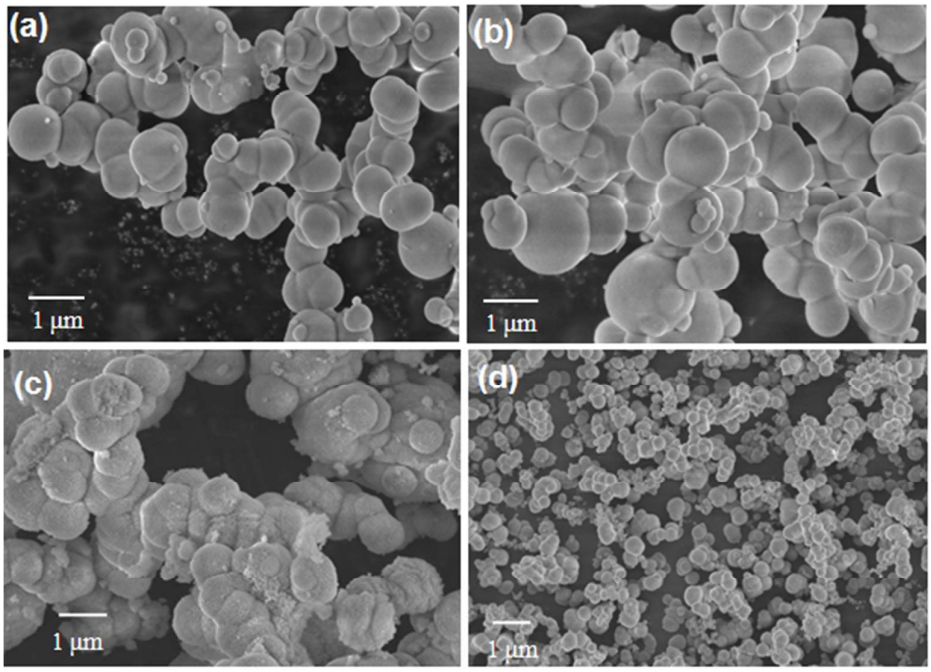

Fig. 2 FESEM images of ZnS microspheres, **S1** (a), **S2** (b), **S3** (c) and **S4** (d) showing the spherical morphology.

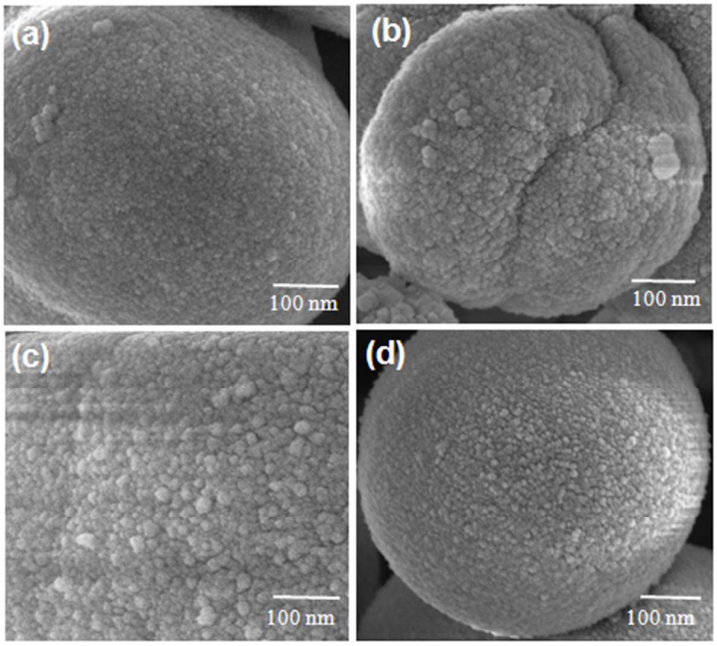

Fig. 3 FESEM images of the surface of ZnS microspheres **S1** (a), **S2** (b), **S3** (c) and **S4** (d) showing the presence of NCs.

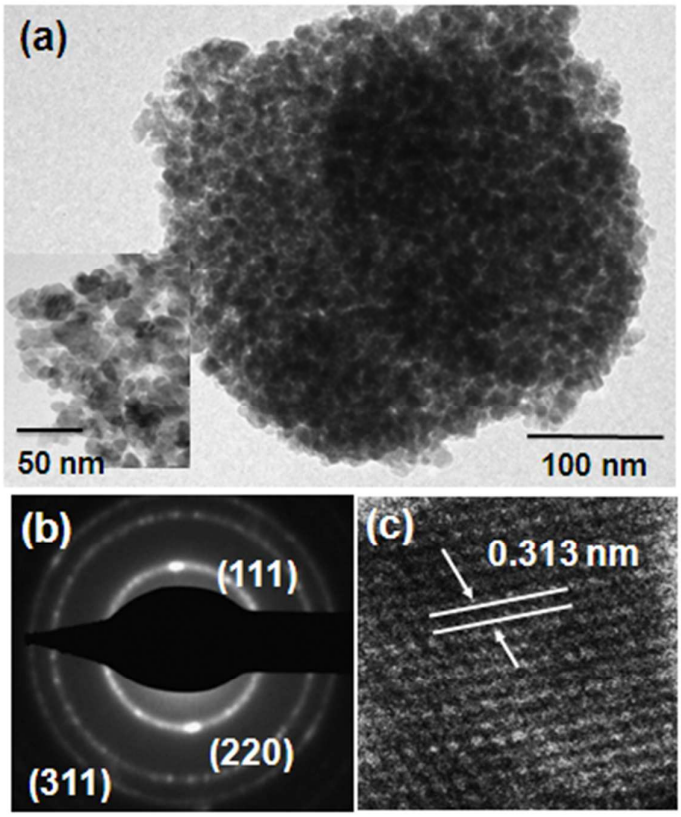

Fig. 4 (a) TEM image of uncapped ZnS microspheres **S3** showing a single ZnS microsphere (inset: magnified image showing the presence of NCs), (b) and (c) shows the SAED pattern and the lattice fringe of ZnS respectively.

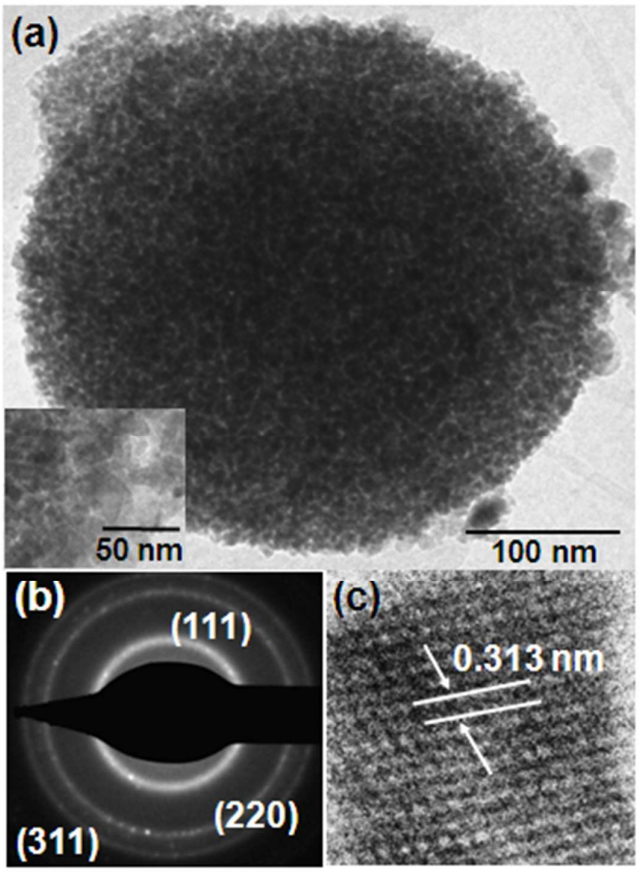

Fig. 5 (a) TEM image of MCE-capped ZnS microspheres **S4** showing a single microsphere, (inset shows magnified image of the surface of the microsphere showing the presence of ZnS NCs). (b) and (c) shows the SAED pattern and lattice fringe of ZnS respectively.

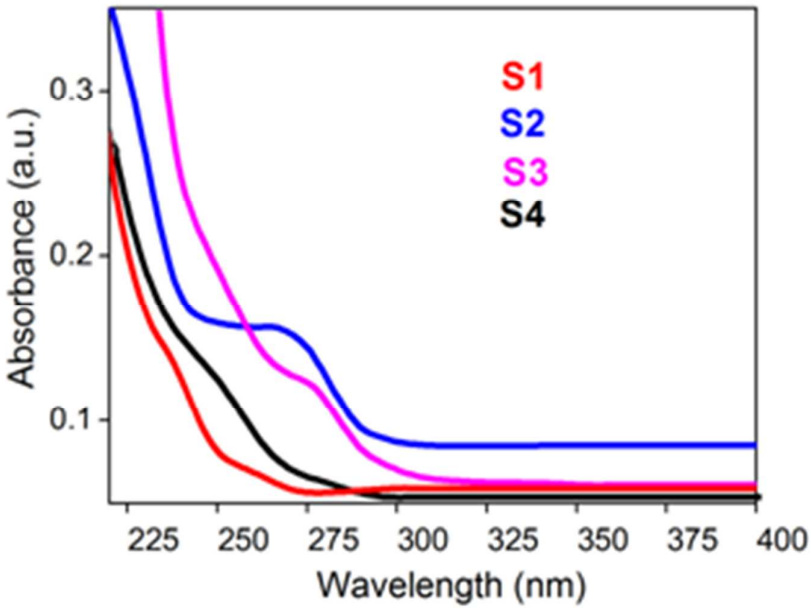

Fig. 6 UV-vis absorption spectra of the ZnS microspheres **S1-S4** in methanol.

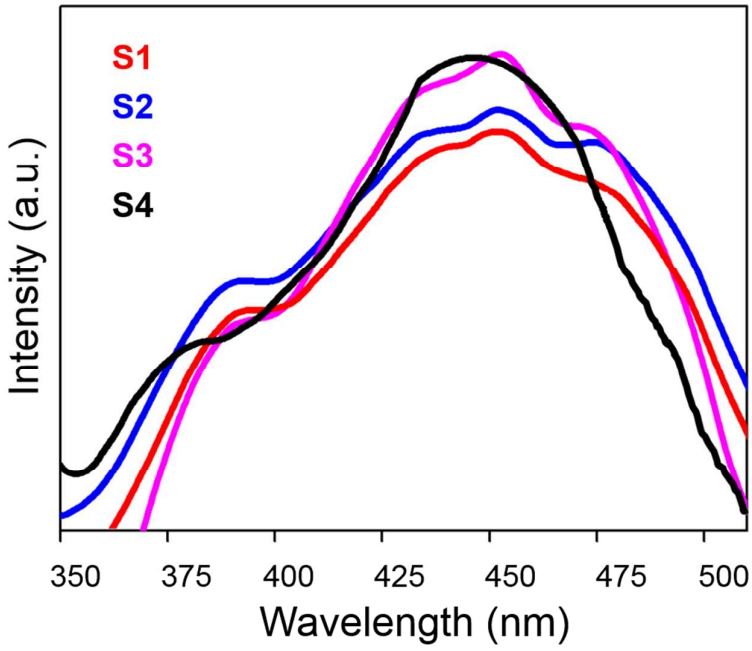

Fig. 7 Photoluminescence spectra of ZnS microspheres **S1-S4** in methanol .

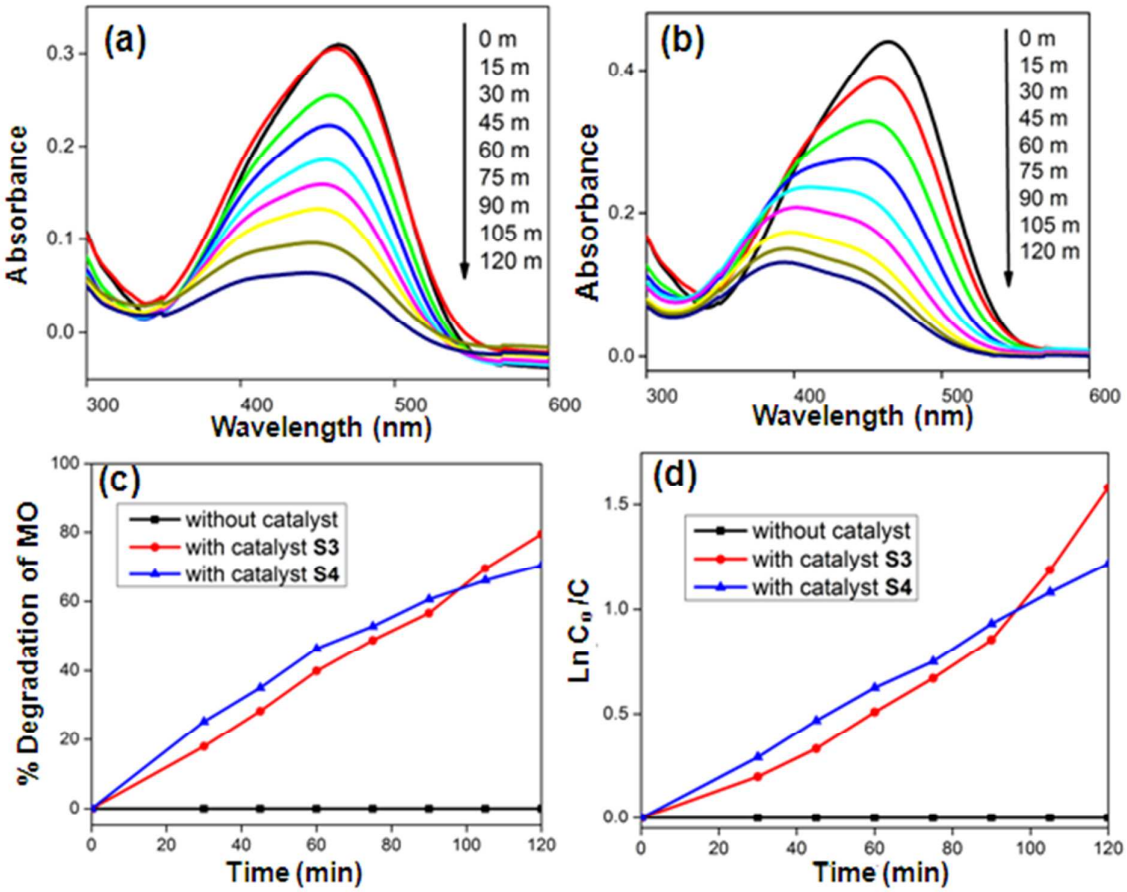

Fig.8 Time-dependent UV–vis absorption spectra for degradation of MO (5.0×10^{-5} M in 50 mL H_2O) using ZnS (40 mg) microspheres (**S3**) (a) and **S4** (b) under UV light, (c) percentage conversion of MO with time and (d) plot of $\ln(C_o/C)$ with time.

For graphical abstract

A facile, one-pot solvothermal method for syntheses of template-free ZnS microspheres composed of nanocrystals (~ 3-6 nm) using $(C_7H_7)S_2$ as a new in situ source of S^{2-} ions without and with the use of MCE-capping agent has been demonstrated. Photocatalytic investigation of the microspheres revealed very good activity for degradation of MO under UV light irradiation.